Journal of Hydrology 561 (2018) 987–999

Contents lists available at ScienceDirect

Journal of Hydrology

journal homepage: www.elsevier.com/locate/jhydrol

Research papers

The Gaussian copula model for the joint deficit index for droughts

H. Van de Vyver*, J. Van den Bergh*

Royal Meteorological Institute of Belgium, Ringlaan 3 Avenue Circulaire, B-1180 Brussels, Belgium

A R T I C L E I N F O

This manuscript was handled by A. Bardossy, Editor-in-Chief, with the assistance of Anne-Catherine Favre, Associate Editor

Keywords:
Drought
Joint deficit index
Gaussian copula
Geostatistics

A B S T R A C T

The characterization of droughts and their impacts is very dependent on the time scale that is involved. In order to obtain an overall drought assessment, the cumulative effects of water deficits over different times need to be examined together. For example, the recently developed joint deficit index (JDI) is based on multivariate probabilities of precipitation over various time scales from 1- to 12-months, and was constructed from empirical copulas. In this paper, we examine the Gaussian copula model for the JDI. We model the covariance across the temporal scales with a two-parameter function that is commonly used in the specific context of spatial statistics or geostatistics. The validity of the covariance models is demonstrated with long-term precipitation series. Bootstrap experiments indicate that the Gaussian copula model has advantages over the empirical copula method in the context of drought severity assessment: (i) it is able to quantify droughts outside the range of the empirical copula, (ii) provides adequate drought quantification, and (iii) provides a better understanding of the uncertainty in the estimation.

1. Introduction

Drought is a major natural hazard with a serious impact on human societies and ecosystems. At least 11% of the European population and 17% of its territory have been affected by water shortage, and the total cost of droughts in Europe over the past thirty years is estimated at EUR 100 billion (EEA, 2009). A review of drought definitions is given in Wilhite and Glantz (1985), where four different drought types are identified: meteorological, hydrological, agricultural, and socio-economic drought. Drought severity can be assessed with indices that are updated at regular times, and are based on present meteorological or hydro-meteorological conditions. For example, the widely used Palmer drought severity index (Palmer, 1965) uses available precipitation and temperature data. Another example is the standardized precipitation index (SPI) of McKee et al. (1993), which has been recommended by the World Meteorological Organization (WMO, 1985) as the primary meteorological drought index to be used.

Because drought-related impacts can be complex, drought monitoring based on a single variable or index may be inadequate. During the past decades, a lot of attention has been paid to the combined use of multiple drought-related variables and indices for overall drought assessment. We refer to Hao and Singh (2015) for an exhaustive review. For example, the U.S. drought monitor (Svoboda, 2002), produces maps of the overall drought condition, and these are based on the integration of multiple drought indices. The use of multivariate distributions for drought risk assessment is a relatively new development (Beersma and Buishand, 2004; Kao and Govindaraju, 2010). The joint deficit index (JDI) of Kao and Govindaraju (2010) is a multivariate probability-based drought index at time scales from 1- to 12-months.

In Kao and Govindaraju (2010), it was argued that empirical copulas for the 12-dimensional structure are reliable when the record lengths are quite large (say, more than 100 years). However, high quality long-term series are scarce, and it would be advantageous to have a flexible copula method at our disposal that extends consistently to shorter series. This motivates us to investigate the performance of parametric copula models. We use a Gaussian copula model for the JDI, in which the covariance matrix is specified by a flexible two-parameter function. We show that the dependence structure across the time scales can be greatly simplified by reformulating the problem in terms of the covariance functions from the methodology of spatial statistics.

2. Drought definitions

2.1. Standardized precipitation index (SPI)

The SPI was introduced by McKee et al. (1993), and is widely used to characterize meteorological droughts over a range of time scales (e.g. 3-, 6-, 9-, 12-, 24-months). Let D_i be the total precipitation of a certain month, and the accumulated values

$$x_w^{(m)} = \sum_{i=m-w+1}^{m} D_i, \tag{1}$$

* Corresponding authors.
E-mail addresses: hvijver@meteo.be (H. Van de Vyver), jorisvdb@meteo.be (J. Van den Bergh).

https://doi.org/10.1016/j.jhydrol.2018.03.064
Received 17 January 2018; Received in revised form 13 March 2018; Accepted 25 March 2018
Available online 05 April 2018
0022-1694/

present the w-monthly precipitation with respect to month m. The main idea of McKee et al. (1993) is to express drought severity in terms of the probability of the observed precipitation depth $x_w^{(m)}$. Let the precipitation depths be a realization of the random variable X_w, and F_{X_w} the cumulative distribution function, i.e. $F_{X_w}(x_w^{(m)}) = \Pr\{X_w \leqslant x_w^{(m)}\}$. As is well known, $U_w = F_{X_w}(X_w)$ is uniformly distributed on the interval [0,1]. Given the input variable $x_w^{(m)}$, the SPI at time scale w is computed by:

$$\mathrm{SPI}_w = \phi^{-1}(u_w), \tag{2}$$

where $u_w = F_{X_w}(x_w^{(m)})$ is the uniform transformed input variable, and ϕ is the standard normal CDF. As suggested by McKee et al. (1993), F_{X_w} can be modeled by a two-parameter Gamma distribution. The cases $\mathrm{SPI}_w > 0$, $\mathrm{SPI}_w < 0$, and $\mathrm{SPI}_w = 0$ indicate wet, dry, and normal conditions, respectively, for the w-month window. The SPI can be applied in a similar way to snowpack (Staudinger et al., 2014), streamflow (Nabaltis and Tsakiris, 2009), soil moisture (Sims et al., 2002), and ground water (Bloomfield and Marchant, 2013).

2.2. Joint deficit index (JDI)

Kao and Govindaraju (2010) propose an overall characterization of droughts by examining various temporal scales together by means of multivariate probabilities. Given accumulated precipitation $(x_1^{(m)},\ldots, x_{12}^{(m)})$ with respect to a certain month, and over 12 different time scales (1-, …, 12 months), we need to estimate the multivariate probability $\Pr\{X_1 \leqslant x_1^{(m)},\ldots, X_{12} \leqslant x_{12}^{(m)}\}$. The influence of marginal aspects on the dependence structure between X_w's, can be removed by transformation to uniform margins, i.e. $\Pr\{X_1 \leqslant x_1^{(m)},\ldots, X_{12} \leqslant x_{12}^{(m)}\} = \Pr\{U_1 \leqslant u_1^{(m)},\ldots, U_{12} \leqslant u_{12}^{(m)}\}$, and observing that there is a unique function C such that:

$$\Pr\{U_1 \leqslant u_1^{(m)},\ldots, U_{12} \leqslant u_{12}^{(m)}\} = C(u_1^{(m)},\ldots, u_{12}^{(m)}). \tag{3}$$

The function C is the copula (Nelsen, 2006); it contains complete information about the joint distribution, apart from the marginal distributions. The Kendall distribution function

$$K_C(q) = \Pr\{C(U_1,\ldots, U_{12}) \leqslant q\}, \tag{4}$$

maps multivariate data into one single value. For a given $q = C(u_1^{(m)},\ldots, u_{12}^{(m)})$, the JDI is defined as

$$\mathrm{JDI} = \phi^{-1}(K_C(q)). \tag{5}$$

Kao and Govindaraju (2010) employed empirical copulas, which are defined as follows. Given n transformed data points $\mathbf{u}_i = (u_{1,i},\ldots, u_{12,i})$, $i = 1,\ldots, n$, the corresponding empirical copula is defined as (Nelsen, 2006):

$$\widehat{C}_n(u_1,\ldots, u_{12}) = \frac{1}{n}\sum_{i=1}^{n} \mathbb{1}(u_{1,i} \leqslant u_1,\ldots, u_{12,i} \leqslant u_{12}). \tag{6}$$

However, extreme droughts, which are outside the observational range cannot be quantified with empirical copulas. Examples of parametric copulas, such as the Student t-copula and Gaussian copula, are provided in the Appendix of Kao and Govindaraju (2010). Their results suggested that both copulas perform similarly for precipitation JDIs. Since the evaluation of t-Student copulas is time consuming, we selected the Gaussian copula in our study.

3. The Gaussian copula model

The Gaussian copula C_G can be expressed as

$$C_G(u_1,\ldots, u_{12}\,|\,\Sigma) = \Phi_\Sigma(\phi^{-1}(u_1),\ldots, \phi^{-1}(u_{12})), \tag{7}$$

with Φ_Σ, the multivariate Gaussian CDF with zero mean and positive definite covariance matrix Σ. From Eq. (2), it follows that the Gaussian copula model for the JDI is the joint probability for the SPIs at time scales 1-, …, 12 months.

The covariances can be estimated empirically from the data. However, this does not ensure a positive definite resulting covariance matrix (Renard and Lang, 2007). Furthermore, empirical estimations can be physically inconsistent: it may happen that for some elements $\rho_{w,w'}$ of Σ, the estimations satisfy $\widehat{\rho}_{w,w'} < \widehat{\rho}_{w,w''}$ for $w < w' < w''$, in particular for shorter series.

Our main aim is to overcome these issues by parameterizing the covariance matrix with a specified model. We accomplish this by using covariance functions that are known to be positive definite, and are commonly used in spatial statistics and geostatistics (Cressie, 1993; Diggle and Ribeiro, 2007). We extend the random process $Y_w = \phi^{-1}(F_{X_w}(X_w))$, to a continuous spatio-temporal random process $Y(w,t)$ as a function of accumulation time w, and accumulation end time t. Since w is expressed in months, and the number of days differs from month to month, we define a month as a 30 day-period in the model derivation. To make the connection with spatial statistics, we view $Y(w,t)$ as a random process at 'location' w. See Appendix A for a general description of random fields. A common simplifying assumption for stationary spatial random fields is isotropicity, which means that the spatial covariance structure depends only on the distance between two locations. In practical applications, one mostly uses the Euclidean distance, but this can never be suited for the present application. It seems a reasonable assumption that the correlation between monthly and 2-monthly totals, should be approximately equal to the correlation between 3-monthly and 6-monthly precipitation depths, and so forth. Therefore, we propose the logarithmic distance between w and w':

$$h = |\log(w) - \log(w')|, \tag{8}$$

as a candidate model. In Section 6.1, the hypothesis that the covariance $\mathrm{Cov}[Y(w,t), Y(w',t)]$ depends only on the logarithmic distance, is shown to be statistically significant, at least for w-values within the practical range (e.g. from 1- to 12 months). This is equivalent to the assumption

$$\mathrm{Cov}[Y(kw,t), Y(kw',t)] = \mathrm{Cov}[Y(w,t), Y(w',t)]. \tag{9}$$

We denote by $\rho(h) := \mathrm{Cov}[Y(w,t), Y(w',t)]$, the covariance function. We summarize the commonly used standard covariance functions (Cressie, 1993; Diggle and Ribeiro, 2007):

- *The Matérn family:*

  $$\rho(h) = \{2^{\kappa-1}\Gamma(\kappa)\}^{-1}(h/\sigma)^{\kappa}K_\kappa(h/\sigma), \quad \sigma > 0, \quad \kappa > 0, \tag{10}$$

  in which $K_\kappa(.)$ denotes a modified κth-order Bessel function, σ is the scale parameter, and κ is the shape parameter.
- *The powered exponential family:*

  $$\rho(h) = \exp(-(h/\sigma)^{\kappa}), \quad \sigma > 0, \quad 0 < \kappa \leqslant 2, \tag{11}$$

- *The exponential family:*

  $$\rho(h) = \exp(-h/\sigma), \quad \sigma > 0, \tag{12}$$

  which is a particular case of the Matérn and powered exponential family for $\kappa = 0.5$, and $\kappa = 1$, respectively.

4. Variogram-based estimation

The variogram of the stochastic process $Y(w,t)$ is

$$\gamma(w,w') = \frac{1}{2}\mathrm{Var}[Y(w,t) - Y(w',t)]. \tag{13}$$

For the isotropic case, and given that $\mathrm{Var}[Y(w,t)] = 1$, Eq. (13) simplifies to

$$\gamma(h) = 1 - \rho(h). \tag{14}$$

It can be seen that the variogram and the covariance function are theoretically equivalent, but a variogram-based analysis offers a number of advantages, especially when the data locations form an irregular design, for details see Cressie (1993), Diggle and Ribeiro (2007).

Given n transformed data points $\mathbf{y}_i = (y_{1,i},\ldots, y_{12,i})$, $i = 1,\ldots, n$, the empirical variogram is given by

$$\hat{\gamma}(w, w') := \frac{1}{2n}\sum_{i=1}^{n}(y_{w,i}-y_{w',i})^2, \tag{15}$$

which, for an isotropic model, results in

$$\hat{\gamma}(h) = \frac{1}{|N_h|}\sum_{(w,w')\in N_h}\hat{\gamma}(w, w'), \tag{16}$$

where N_h denotes the set of pairs (w, w') such that the distance equals h, and $|N_h|$ is the number of pairs in the set N_h.

Parameter estimation of the correlation functions, Eqs. (10)–(12), is performed with the ordinary least squares method. This estimates the parameters θ to minimize the objective function

$$S(\theta) = \sum_{k=1}^{\tilde{n}}(\hat{\gamma}(h_k)-\gamma(h_k;\theta))^2, \tag{17}$$

where $\gamma(h;\theta)$ is the theoretical variogram, and $\tilde{n}$ the number of different h-values.

Model selection criteria are needed to decide which covariance model, Eqs. (10)–(12), should be preferred. We use the Akaike Information Criterion (AIC), defined as:

$$\mathrm{AIC} = 2n_p + \tilde{n}\ln S(\hat{\theta}), \tag{18}$$

where n_p is the number of model parameters. The best model has the lowest AIC-value.

5. Data

We selected four high quality long-term daily precipitation series, with at least 100 years of data. The stations are located in: Uccle (Belgium), Marseille (France), Milan (Italy), and St. Petersburg (Russian Federation). The Uccle series was collected by the Royal Meteorological Institute of Belgium (RMI), and the other series were obtained from the European Climate Assessment & Dataset (Klein Tank et al., 2002). We summarize the station characteristics in Table 1.

As in Kao and Govindaraju (2010), when fitting the marginal distributions of X_w, the problem of auto-correlation and seasonal variability in the data can be resolved by collecting $x_w^{(m)}$ annually for each month. The 2-parameter Gamma distribution was fitted to $x_w^{(m)}$ separately for each w and each month. The goodness-of-fit was assessed with the Cramer-von Mises test, the Anderson–Darling test and the Kolmogorv-Smirnov test at the 5% significance level. It was found that the Kolmogorv-Smirnov test only rejected two accumulated series ($w = 5$ and $w = 6$ for the month September, station Uccle). Consequently, the tests lend support to the 2-parameter Gamma model for the marginals. Next, once a distribution $F_{X_w^{(m)}}$ was fitted to $x_w^{(m)}$, the application of the transformation $u_w^{(m)} = F_{X_w^{(m)}}(x_w^{(m)})$, results in uniform transformed data points $\mathbf{u}_i = (u_{1,i},\ldots, u_{12,i})$, with $i = 1,\ldots, 12\times n_y$ (n_y: number of years). Finally, normally transformed data $\mathbf{y}_i = \phi^{-1}(\mathbf{u}_i)$ was obtained.

Table 1
Long term precipitation stations. RMI: Royal Meteorological Institute of Belgium. ECA&D: European Climate Assessment & Dataset (Klein Tank et al., 2002).

Place	Latitude	Longitude	Alt. (m a.s.l.)	Years	Provided by
Uccle	50°47′55″	4°21′29″	100	1898–2015	RMI
Marseille	43°18′18″	5°23′48″	75	1881–2004	ECA&D
Milan	45°28′18″	9°11′21″	150	1858–2008	ECA&D
St. Petersburg	59°58′00″	30°18′00″	3	1881–2013	ECA&D

6. Results and discussion

6.1. Isotropicity

As explained in Appendix A, to check the isotropicity of one-dimensional random fields, it is sufficient to test for stationarity. We used the test of Jun and Genton (2012) for stationarity of spatial or spatio-temporal fields. They considered cases where the spatial domain is planar or spherical, but the results also apply to one-dimensional domains. The basic idea is described in Appendix A, and consists of dividing the spatial domain into two disjoint domains, and to use the test statistic that is based on the differences between empirical estimators of covariances at given lags from the sub-domains. The actual dataset consists of 12 series of normally transformed accumulated precipitation depths (1-,…,12 months), which, however, do not give a sufficient number of pairs whose points share the same distance. Therefore, we extend the dataset to accumulation times $w = 25, 30, 35, \ldots, 365$ days, where accumulation end times correspond with the end of a month. This gives rise to 69 series of normally transformed accumulated precipitation depths. We consider 1000 randomly sampled divisions of two disjoint domains. For each division, we search for h-values for which there are a sufficient high number of pairs whose points have distance h. In the terminology of Appendix A, this defines space–time lags $k = (h, u)$. We only consider time lag $u = 0$, because we are only concerned with spatial covariances. Next, we compute the test statistic $\mathscr{T}_l$, Eq. (A.3), where l refers to the number of lags. Jun and Genton (2012) proved that $\mathscr{T}_l$ is asymptotically χ^2-distributed with degrees of freedom l, under the null hypothesis that the random field is stationary. It turned out that for the following percentage of the different divisions, stationarity was accepted at the 5% significance level: 92.3% (Uccle), 93.7% (Marseille), 93.3% (Milan) and 91.7% (St. Petersburg).

6.2. Estimation and validation

The estimation results listed in Table 2 indicate that the powered exponential covariance model is the best choice. The empirical and theoretical variogram are shown in Fig. 1. The corresponding covariance matrices are given in Tables B.6 and B.7 of Appendix B. It can be seen that for Uccle and St. Petersburg, the precipitation marginals have a comparable level of temporal correlation. On the other hand, in Marseille, the correlation decays faster for increasing h-values. The case of Milan tends to be in the middle of the two.

The goodness-of-fit was assessed by comparing the empirical copula with the Gaussian copula, evaluated at the transformed data points $\mathbf{u}_i = (u_{i,1},\ldots, u_{i,12})$, $i = 1,\ldots, n$. Denote by $\hat{\Sigma}$ the estimated covariance matrix, and $\hat{C}_G(\mathbf{u}_i) := C_G(\mathbf{u}_i|\hat{\Sigma})$, the estimated Gaussian copula. The goodness-of-fit can be visualized by plotting the empirical copula $\hat{C}_n(\mathbf{u}_i)$ against the Gaussian copula $\hat{C}_G(\mathbf{u}_i)$, $i = 1,\ldots, n$, see Fig. 2. The model works well, because the points lie close to the unit diagonal. To have an idea of the overall performance, we used the following goodness-of-fit scores (Table 3): mean absolute error (MAE), root mean squared error (RMSE), BIAS, and maximum error (MAX). Kao and Govindaraju (2010) reported a RMSE of 0.0083 for the Gaussian copula (with empirically estimated covariances), which is of the same order of magnitude.

6.3. Sensitivity to sample size

The advantage of a parametric copula method is that it should extend in a consistent way to shorter data series. Having confirmed the validity of the new method for long-term series, we now evaluate the effect of the data size on the estimation. Ideally, one needs at least 20–30 years of monthly values for the SPI-calculation, with

Table 2
Parameter estimation of the correlation functions, Eq. (10)–(12). Lowest AIC-values are indicated in bold.

Matérn				Powered Exponential				Exponential		
$\hat{\sigma}$	$\hat{\kappa}$	$S(\hat{\sigma},\hat{\kappa})$	AIC	$\hat{\sigma}$	$\hat{\kappa}$	$S(\hat{\sigma},\hat{\kappa})$	AIC	$\hat{\sigma}$	$S(\hat{\sigma})$	AIC
Uccle										
1.981	0.553	1.8e−3	−281.13	2.141	1.063	1.6e−3	**−285.13**	2.215	5.0e−3	−236.27
Marseille										
1.825	0.485	1.7e−3	−284.19	1.783	0.980	1.6e−3	**−286.98**	1.767	2.0e−3	−277.64
Milan										
1.954	0.500	2.7e−3	−261.84	1.959	0.996	2.7e−3	−262.08	1.955	2.7e−3	**−263.84**
St. Petersburg										
2.068	0.530	1.0e−3	−306.02	2.162	1.035	9.8e−4	**−307.87**	2.205	2.1e−3	−275.69

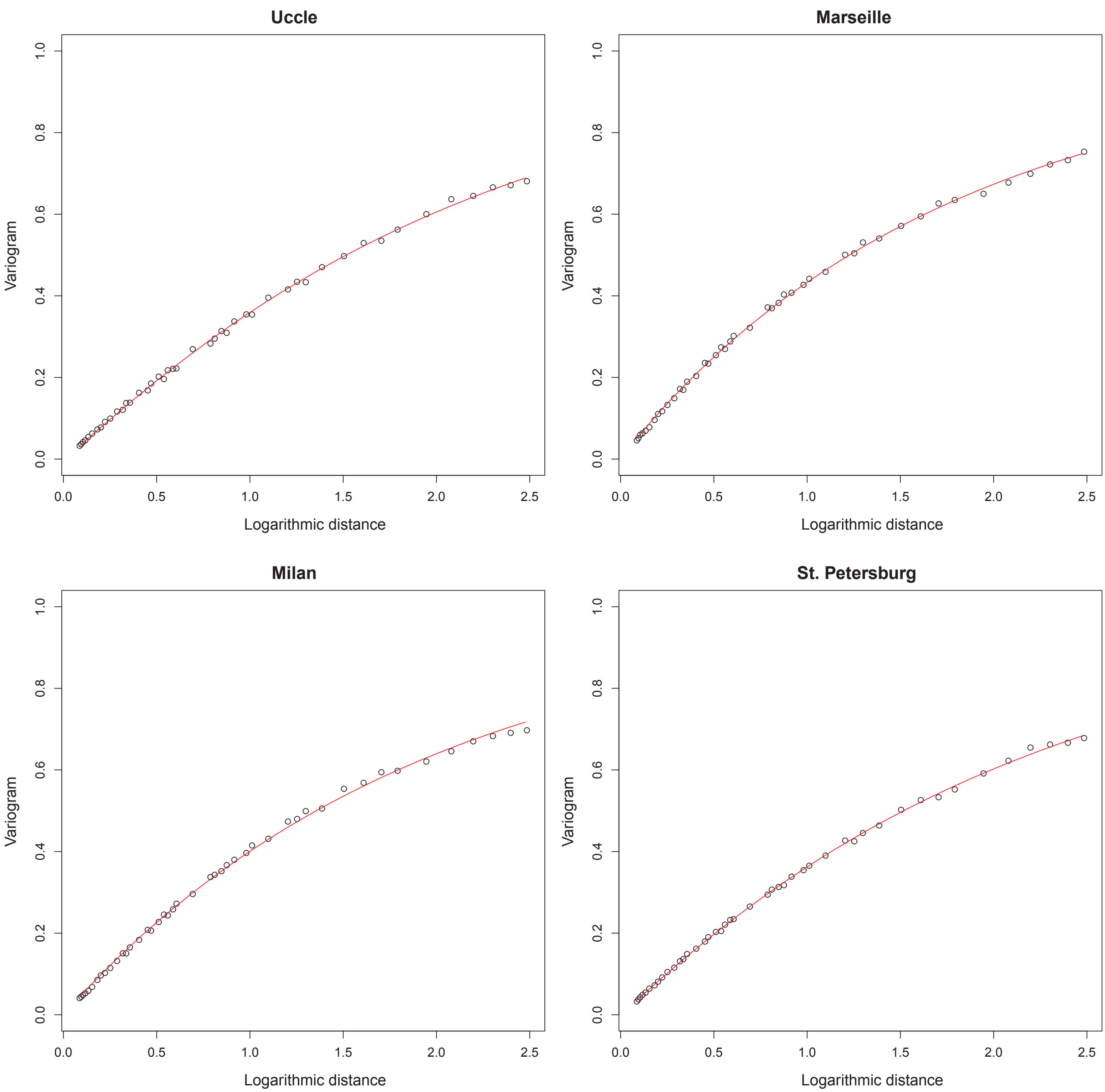

Fig. 1. Variogram with standard normal marginals. *Dots:* empirical variogram. *Solid line:* theoretical variogram.

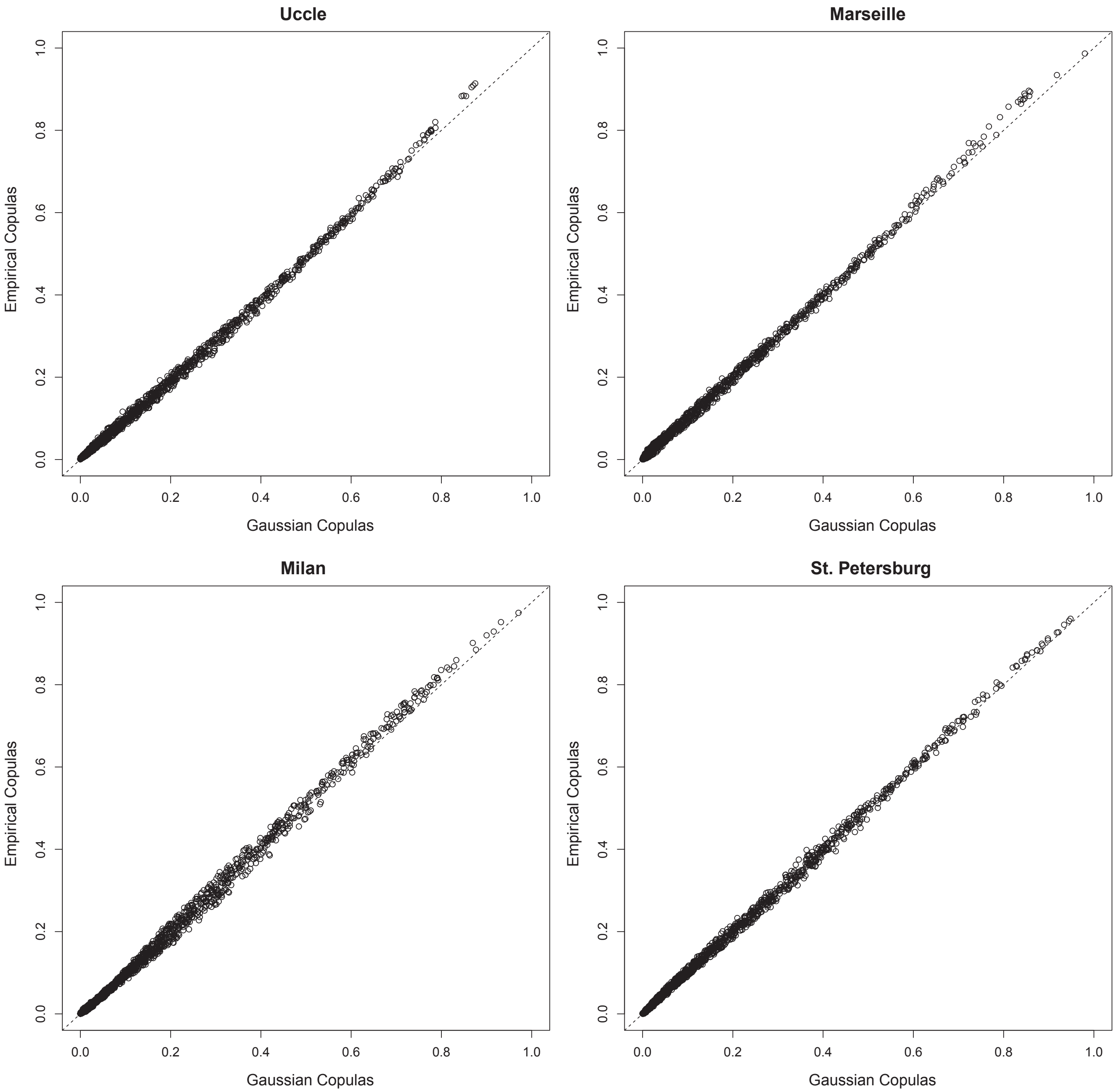

Fig. 2. Goodness-of-fit plots. Empirical copulas versus Gaussian copulas. *Dash line:* leading diagonal.

Table 3
Goodness-of-fit scores for the Gaussian copula model.

	MAE	RMSE	BIAS	MAX
Uccle	7.42e−3	1.04e−2	−4.15e−3	3.88e−2
Marseille	6.01e−3	8.30e−3	2.01e−3	4.66e−2
Milan	7.78e−3	1.15e−2	8.35e−5	4.78e−2
St. Petersburg	5.35e−3	7.52e−3	8.79e−4	3.50e−2

50–60 years (or more) being optimal and preferred (WMO, 1985). The two main sources of uncertainty in the new methodology are estimation of (i) the margins, and (ii) the dependence structure between the margins. We applied a bootstrap procedure to calculate measures of uncertainty associated with the correlation functions. A bootstrap sample was obtained by resampling of the years (with replacement) from a subseries of the original dataset (e.g. the last 30 years, 40 years, …). For each sample, an estimate of the parameters, $\hat{\sigma}$ and $\hat{\kappa}$, was computed. This process was repeated a large number of times (typically 10^3 or 10^4 times), which provided a sample distribution of the parameter estimates. Given a significance level α, the $(1-\alpha)$-confidence bounds are then the $\alpha/2$- and $(1-\alpha/2)$-quantiles of the sample distribution. A commonly used level is $\alpha = 0.05$. In Fig. 3, we show the covariance parameter estimates as a function of the number of years of data. In addition, the 0.95-confidence intervals are plotted. The bootstrap methodology also directly provided uncertainty estimates for the powered exponential correlation function $\rho(h)$, see Fig. 4 for the case $h = 2$. It can be seen that for time windows larger than 40–60 years, the estimations are more or less stable.

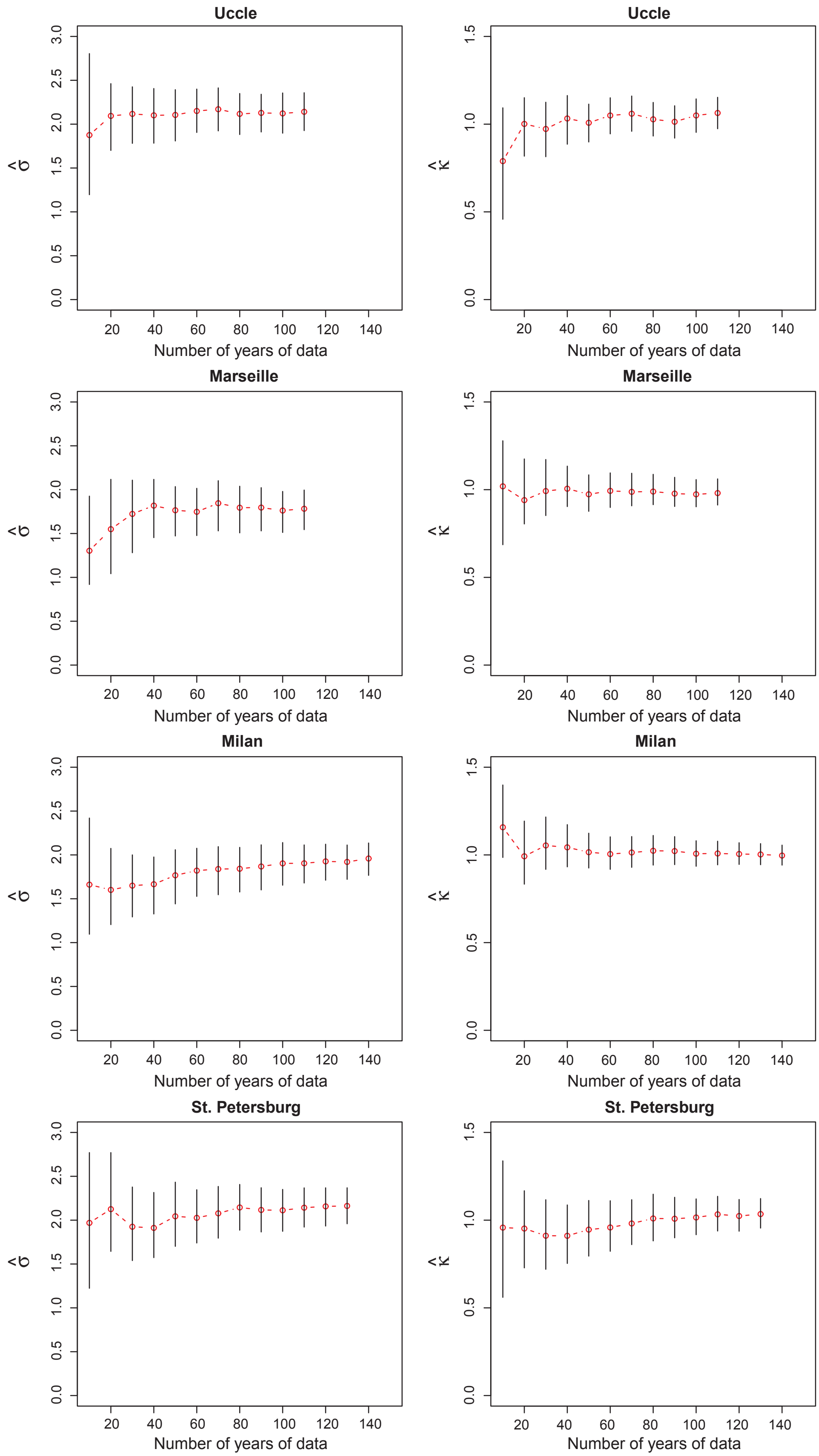

Fig. 3. Parameter estimates ($\hat{\sigma}$ and $\hat{\kappa}$) of the powered exponential correlation function, Eq. (11), as a function of the number of years of data. Vertical lines are the 0.95-confidence intervals.

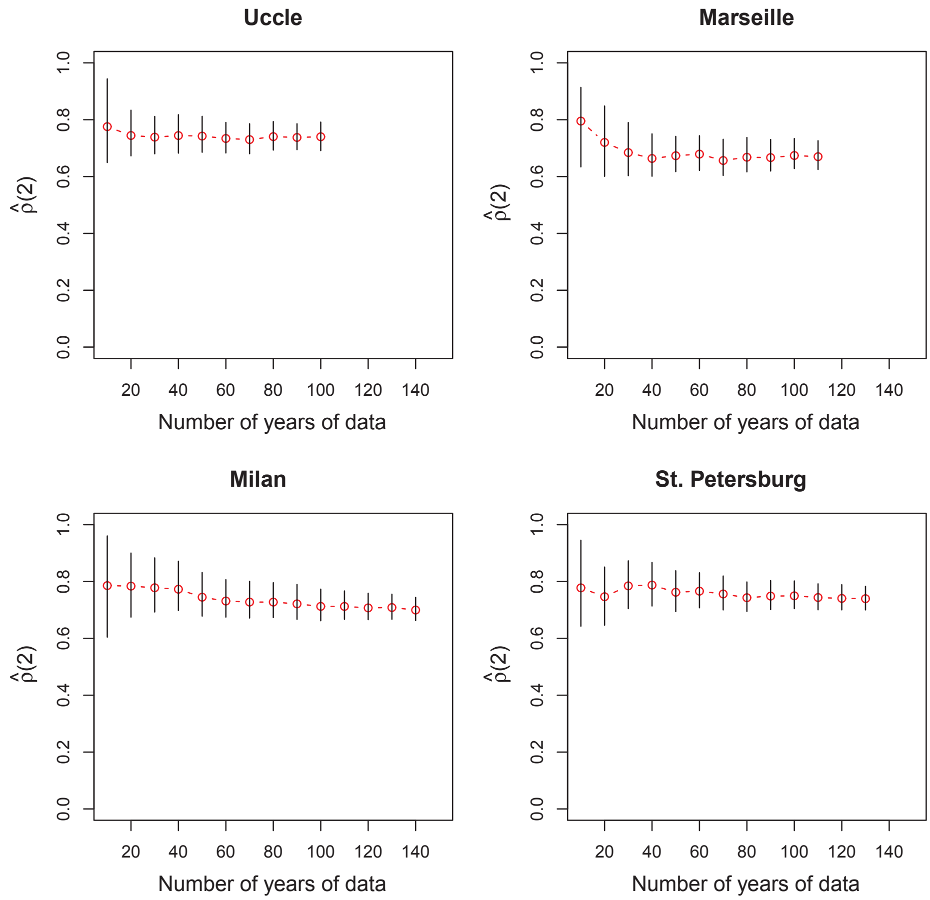

Fig. 4. Estimates of the powered exponential correlation function $\rho(h)$, Eq. (11), for $h = 2$, as a function of the number of years of data. Vertical lines are the 0.95-confidence intervals.

Table 4
Drought monitor classification of Svoboda (2002).

Category	Drought condition	Probability of occurrence (%)	Normal quantiles
D0	Abnormally dry	20–30	-0.84 to -0.52
D1	Moderate drought	10–20	-1.28 to -0.84
D2	Severe drought	5–10	-1.64 to -1.28
D3	Extreme drought	2–5	-2.05 to -1.64
D4	Exceptional drought	2	-2.05

6.4. Drought category estimation: Empirical versus Gaussian copula

We consider the categories used in the U.S. drought monitor (Svoboda, 2002). This includes abnormally dry (D0), moderate drought (D1), severe drought (D2), extreme drought (D3), and exceptional drought (D4). Table 4 shows the range of SPI values along with their probabilities of occurrence and corresponding drought conditions, see also Kao and Govindaraju (2010). We assessed and compared the ability of the copula models to categorize droughts as follows. According to the usual practice, the dataset on which the copula model is fitted (i.e. the training set), is different from the dataset on which the fitted model calculates the JDI-values (i.e. the validation set). We considered the entire long-term precipitation series (Table 1) as the validation set. The resampled series, obtained in Section 6.3, were used here as training sets. Finally, for each copula model, we counted how many JDI-values fall into each drought category. We repeated this process 1000 times, and we recorded the average occurrence of the JDI-values per drought category (Fig. 5). The results are shown for 50-year training sets, but other sample sizes (20,…, 100 years) gave nearly the same results. A necessary condition for the copula models to be eligible for drought quantification, is that these percentages correspond to the drought categories D0-D4 (Table 1). Both copulas work sufficiently well for D0-droughts. The more severe the drought, the worse the performance of the empirical copula. In particular, several extreme droughts are outside the range of the resampled empirical copulas, giving rise to undefined JDI-values. To give an idea, a 50-year training set gives, on average, 5–8% undefined JDI-values for the validation set. In contrast, the Gaussian copula works better, but tends to slightly overestimate extreme (D3) and exceptional droughts (D4).

Another important aspect to investigate is the standard error of the JDI-estimations. We selected four drought events in Uccle, each belonging to a different drought category: November 1940 (D1), September 1973 (D2), October 1911 (D3), and September 1959 (D4). The confidence intervals of the corresponding JDI-estimations were obtained through the foregoing resampling procedure. In Fig. 6, we plotted the JDI-estimations as a function of the number of observation years, together with the 0.95-confidence intervals. For series with 40 years of data, or longer, the JDI-estimations appear to be relatively stable. For cases where the drought event was outside the range of the empirical copula, the JDI could not be computed. The greater the drought, or the smaller the dataset, the greater the probability that this

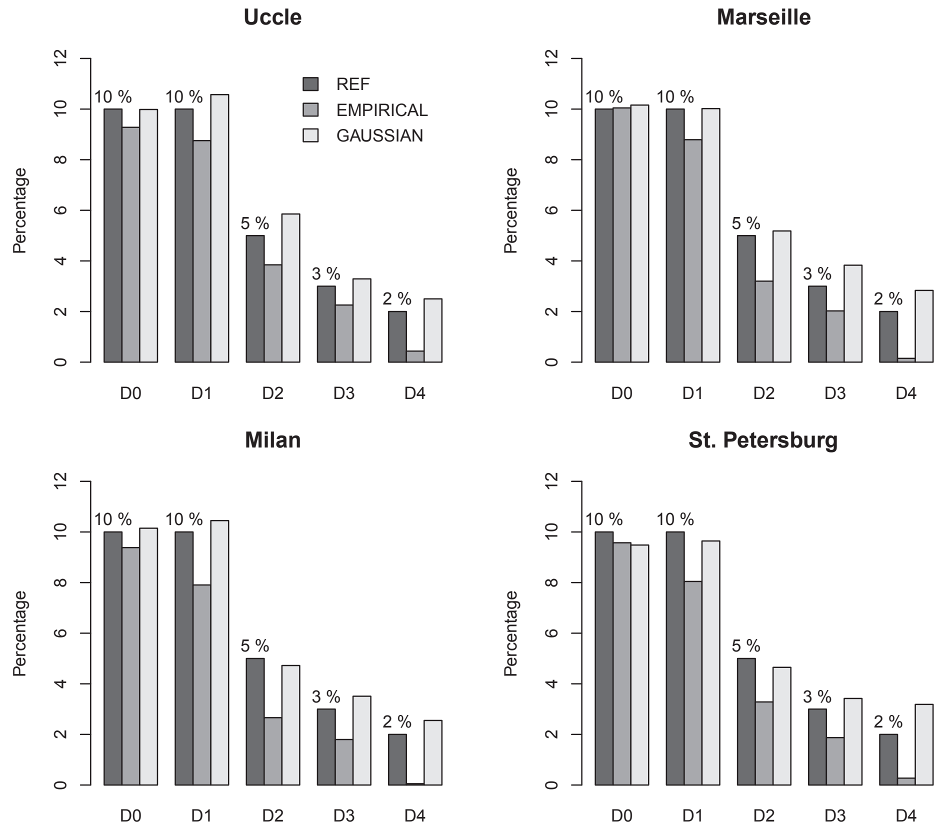

Fig. 5. Number of JDI-values that fall into each drought category, after application of the bootstrap procedure of Section 6.4. "REF" corresponds to the percentage of the given drought category (see Table 4).

will happen. For this reason, it was not always possible to obtain the confidence intervals of the empirical copula-based JDI. In such a case, we tried to gain insight in the degree of uncertainty by using the following criterion: the confidence interval is computed only if less than 10% of the total number of JDI-samples are undefined. The choice of 10% is not motivated by theoretical issues, and is rather arbitrary. In spite of this rule, assessment of uncertainty of the estimation of D0-D1 droughts could only be made for series of moderate length (say 50 year, or longer). For greater droughts, D2-D4, confidence intervals could not be determined. For the Gaussian copula, we can produce confidence intervals without difficulty. Confidence intervals of JDI-estimations are not often entirely contained within one drought category, which may complicate the drought severity assessment. For more than 60 years of data, the confidence intervals are covered by two adjacent drought categories, and sometimes, by a negligible fraction of a third category. Although uncertainties of this order of magnitude are unavoidable, they do not greatly affect the assessment of drought severity.

6.5. A case study for Uccle precipitation

An illustration of the copula-based JDI for the Uccle precipitation series is shown in Fig. 7. We added the normal quantiles of the drought categories to the JDI-plots. We considered both the empirical and Gaussian copulas. The gaps in the graphs (in year 1921, 1986, 1997 and 2007) are associated with undefined empirical copula-based JDI-values. Note that the copulas are fitted on the whole series, so that the training set is equal to the validation set, a situation which is different from the foregoing experiments (an underestimation of severe drought by the empirical copula is thus not to be expected). Here, we investigated whether the D4-droughts agree with major European drought events. Past European drought events from the 1950s to present are discussed in Spinoni et al. (2015). Also, an overview of major European drought events (1959–2007) is contained in the European Drought Reference (EDR) database, which is hosted by the website of the virtual European Drought Centre (EDC, see:www.geo.uio.no/edc). In Table 5, we list the year and JDI-peaks of the D4-drought events (1950–present), and the associated major European droughts. The low JDI-value of April 2007 deserves particular attention. Because the year 2007 was generally a wet year, it could not be related to the 2007-drought of Eastern Europe (see EDR database). The low JDI-value is solely due to the fact that there was, remarkably enough, no precipitation observed during that month. Some major droughts, included in the EDR database, correspond with a less severe classification for Belgium (in terms of the JDI). The summer of 2003, for example, was classified as D1, and thus does not stand out as particularly dry. For the first part of the twentieth century, few authors have examined European drought incidence because instrumental data at high spatial resolution are not available. In van der Schrier et al. (2016), maps of the monthly Palmer drought severity index (PDSI) have been calculated for the period of 1901–2002 for Europe, but they focused on summer moisture variability. For a comparative study, we selected the historical SPI-values of Lloyd-Hughes and Saunders (2002) at various time scales. The driest years, and peak JDI-values (in parenthesis) are: 1899 (−2.66), 1921–1922 (−4.19), 1929 (−2.62), 1933–1934 (−2.25), 1944 (−2.14), 1949 (−2.66), and these dry periods agree well with the low SPI-values of South Dalton, Yorkshire, UK, see Fig. 5 in Lloyd-Hughes and Saunders (2002).

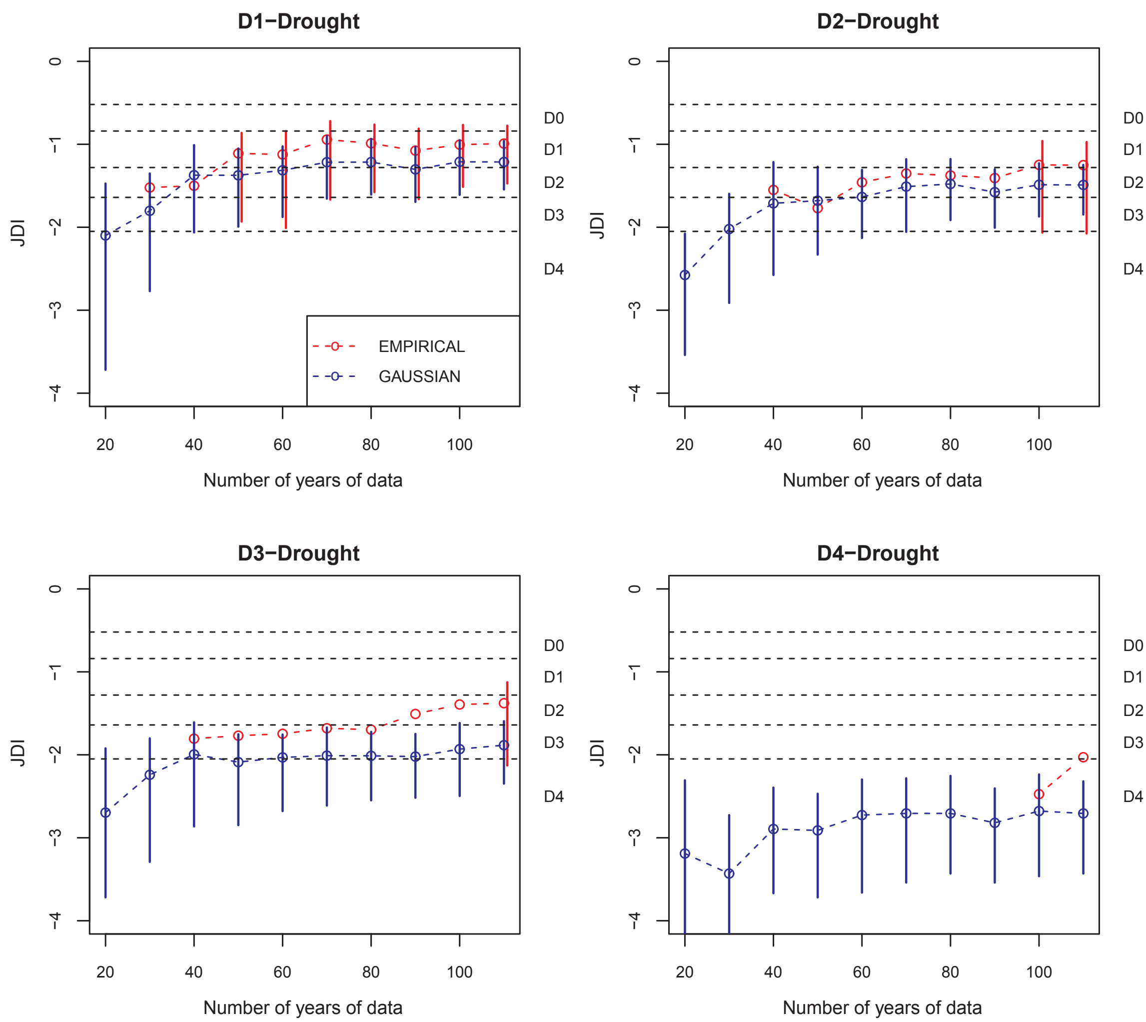

Fig. 6. JDI-estimates, as a function of the number of years of data, for four selected drought events in Uccle. Vertical lines are the 0.95-confidence intervals. D0, …, D4 are the drought categories of Table 4.

7. Conclusion

In this paper, we investigated the possibility to model the JDI for drought characterization by the Gaussian copula model. We developed a parametric model for the covariance matrix of the Gaussian copula. Unlike the sample covariance matrices, the parameterized covariance matrices are consistent and positive definite by construction in our approach. This allows us to apply the model to shorter time series in a consistent way. More specifically, we were able to describe the complex dependence of accumulated precipitation across different temporal scales by a simple and parsimonious model. The main idea is to reformulate the problem as a spatial statistics problem by (i) defining the 'location' of an accumulated rainfall process as the accumulation time, and (ii) considering a suitable 'distance' measure between two accumulation times. We considered a suitable set of covariance functions, with the appropriate properties of being positive definite and monotonically decreasing with the distance. A variogram-based analysis shows an excellent fit of the two-parameter powered exponential (Matérn) family to long-term precipitation data. The computation of Gaussian copulas is cheap, and the new estimation procedure is easy to implement. Sensitivity studies suggest that one needs at least 40–60 years of monthly values for a reliable copula-based JDI-computation.

There are a number of reasons to prefer the Gaussian copula over the empirical copula. First, extreme droughts that are outside the range of the empirical copula cannot be assessed. The greater the drought, or the smaller the dataset, the greater the probability that this will happen. Consequently, bootstrap confidence intervals for JDI-estimations cannot be computed in many situations. Even if 100 year of data were available, confidence intervals for D3-D4 droughts are nearly impossible to define. On the other hand, the parametric Gaussian copula model is able to do so. Secondly, the bootstrap experiments reveal that the empirical copula significantly underestimates the number of occurrences of JDI-values in the drought categories D1-D4. In particular, the most severe droughts (D4) are reproduced exceptionally poorly. The Gaussian copula performs much better for all drought categories, but slightly overestimates D3-D4 droughts.

A case study for Uccle precipitation showed that the D4-droughts, as identified by the JDI, agree well with the major European drought events.

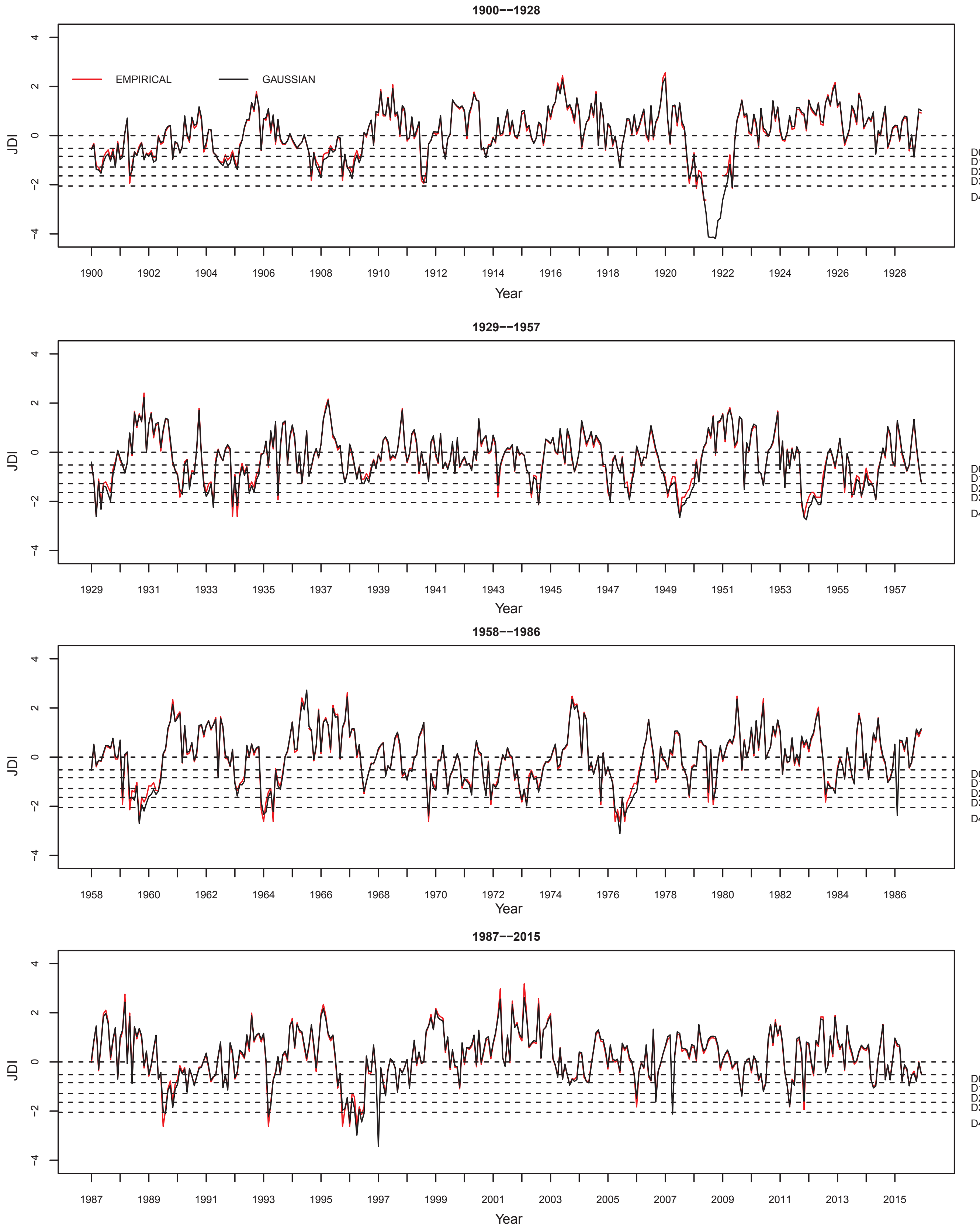

Fig. 7. JDI for Uccle precipitation (1900–2015). D0, …, D4 are the drought categories of Table 4.

Table 5
D4-drought events (1950–present) detected by the JDI (Uccle precipitation), and corresponding major European drought.

Year	JDI at peak	Mentioned by
1953–1954	−2.75	EDR database, Spinoni et al. (2015): Pan-Europe.
1959	−2.70	EDR database, Spinoni et al. (2015): 1959–1960, North-Central-Eastern Europe.
1964	−2.33	Spinoni et al. (2015): North-Central-Eastern Europe.
1969	−2.39	Spinoni et al. (2015): UK-Scandinavia.
1976	−3.11	EDR database, Spinoni et al. (2015): Europe.
1986	−2.37	Spinoni et al. (2015): 1985, South Europe.
1989	−2.09	EDR database, Spinoni et al. (2015): 1989–1991, South Europe.
1993	−2.23	Spinoni et al. (2015): 1992, Central Europe.
1996–1997	−3.45	EDR database, Spinoni et al. (2015): Central and North Europe.
2007	−2.12	

Finally, the study was restricted to precipitation. Future research should indicate if the method can be extended to other variables such as streamflow, precipitation deficit, soil moisture, or snowpack.

Acknowledgements

INDECIS has received funding from EU's H2020 Research and Innovation Program under Grant Agreement number 690462.

Appendix A. A stationarity test for spatio-temporal random fields

We denote a random field as $Z(\mathbf{x})$. For a spatial random field we have $\mathbf{x} = \mathbf{s} \in D$, with D the spatial domain, and for a spatio-temporal random field $\mathbf{x} = (\mathbf{s}, t) \in D \times \mathbb{N}$. In spatial statistics, for example, observations are taken over a 2-dimensional space $D \subset \mathbb{R}^2$ of integer lattice points. Spatio-temporal random field can be used to model spatial data recorded at regular times.

The spatial random field $Z(\mathbf{s})$ is stationary if the mean is constant across the spatial domain, and the covariance is translation invariant. That is $\mathrm{E}[Z(\mathbf{s})] = \mu \in \mathbb{R}$ for all $\mathbf{s} \in D$, and $\mathrm{Cov}[Z(\mathbf{s}), Z(\mathbf{s}+\mathbf{h})] = \mathrm{Cov}[Z(\mathbf{0}), Z(\mathbf{h})] =: \rho(\mathbf{h})$ for all spatial lags $\mathbf{h}$. A stationary spatial random field is isotropic if the covariance depends on the distance alone, i.e. $\rho(\mathbf{h}) = \rho(|\mathbf{h}|)$, where $|.|$ denotes the distance.

A formal test for stationarity of spatio-temporal random fields was proposed by Jun and Genton (2012). They do not require distributional assumptions for the random fields. We briefly discuss the basic idea. For a stationary spatial random field, an estimator of the covariance $\rho(\mathbf{h})$ is

$$\widehat{A}(\mathbf{h};D) = \frac{1}{|S(\mathbf{h};D)|} \sum_{\mathbf{s} \in S(\mathbf{h};D)} Z(\mathbf{s}) Z(\mathbf{s}+\mathbf{h}), \tag{A.1}$$

with $S(\mathbf{h};D) = \{\mathbf{s}\colon \mathbf{s} \in D, \mathbf{s}+\mathbf{h} \in D\}$. Similarly, one can extend Eq. (A.1) for stationary spatio-temporal random field $Z(\mathbf{x})$. For a given space–time lag $\mathbf{k} = (\mathbf{h}, u)$, and n observations in time, we get

$$\widehat{A}(\mathbf{k};D) = \frac{1}{|S(\mathbf{h};D)|(n-u)} \sum_{\mathbf{x} \in S(\mathbf{h};D)} \sum_{t=1}^{n-u} Z(\mathbf{x}) Z(\mathbf{x}+\mathbf{k}). \tag{A.2}$$

Let D_1 and D_2 be non-empty subsets of D with $D = D_1 \cup D_2$. The null hypothesis of stationarity of the random field, is written as $\widehat{A}(\mathbf{k}; D_1) = \widehat{A}(\mathbf{k}; D_2)$. Consider a set Λ of time space-lags, with $|\Lambda| = l$, and compute the vectors (i) $\widehat{\mathbf{G}}_n = (\widehat{\mathbf{G}}_{n,1}, \widehat{\mathbf{G}}_{n,2})^T$ with $\widehat{\mathbf{G}}_{n,i} = \{\widehat{A}(\mathbf{k}; D_i)\colon \mathbf{k} \in \Lambda\}$, $i = 1, 2$, and (ii) $\mathbf{G} = \{\rho(\mathbf{k}), \mathbf{k} \in \Lambda\}$. Under fairly mild conditions, the covariance matrix $\Sigma = \lim_{n\to\infty} n\,\mathrm{Var}(\widehat{\mathbf{G}}_n)$ exists and is finite. For sufficiently large n, we may assume $\Sigma \approx n\,\mathrm{Var}(\widehat{\mathbf{G}}_n)$, so that Σ can be estimated using subsampling. Next, compute the vector $\mathcal{G} = \sqrt{n}\,(\widehat{\mathbf{G}}_n - (\mathbf{G},\mathbf{G})^T)$, and define an $l \times 2l$ matrix $\mathbf{X} = (\mathbf{I}_l, -\mathbf{I}_l)$. Finally, the test statistic for the null hypothesis is

$$\mathscr{T}_l = (\mathbf{X}\mathcal{G})^T (\mathbf{X}\boldsymbol{\Sigma}\mathbf{X}^T)^{-1} \mathbf{X}\mathcal{G}, \tag{A.3}$$

which is asymptotically χ^2-distributed with degrees of freedom l.

Appendix B. Covariance matrices

Table B.6
Correlation coefficient $\rho_{ww'}$ between precipitation marginals y_w and $y_{w'}$. Correlation function: powered exponential family. Upper triangle: Uccle. Lower triangle: Marseille.

w' \ w	1	2	3	4	5	6	7	8	9	10	11	12
1		0.74	0.61	0.53	0.48	0.44	0.41	0.38	0.36	0.34	0.32	0.31
2	0.67		0.84	0.74	0.67	0.61	0.57	0.53	0.50	0.48	0.46	0.44
3	0.54	0.79		0.89	0.80	0.74	0.69	0.65	0.61	0.58	0.56	0.53
4	0.46	0.67	0.85		0.91	0.84	0.79	0.74	0.70	0.67	0.64	0.61
5	0.40	0.59	0.75	0.88		0.93	0.87	0.82	0.78	0.74	0.71	0.68
6	0.37	0.54	0.67	0.79	0.90		0.94	0.89	0.84	0.80	0.77	0.74
7	0.34	0.49	0.62	0.73	0.82	0.91		0.95	0.90	0.86	0.83	0.79
8	0.31	0.46	0.57	0.67	0.76	0.85	0.92		0.96	0.91	0.88	0.84
9	0.29	0.43	0.54	0.63	0.71	0.79	0.86	0.93		0.96	0.92	0.89
10	0.28	0.40	0.51	0.59	0.67	0.75	0.81	0.88	0.94		0.96	0.93
11	0.26	0.38	0.48	0.56	0.64	0.71	0.77	0.83	0.89	0.94		0.97
12	0.25	0.37	0.46	0.54	0.61	0.67	0.73	0.79	0.85	0.90	0.95	

Table B.7
Correlation coefficient $\rho_{ww'}$ between precipitation marginals y_w and $y_{w'}$. Correlation function: powered exponential family. Upper triangle: Milan. Lower triangle: St-Petersburg.

w' \ w	1	2	3	4	5	6	7	8	9	10	11	12
1		0.70	0.57	0.49	0.44	0.40	0.37	0.35	0.33	0.31	0.29	0.28
2	0.74		0.81	0.70	0.63	0.57	0.53	0.49	0.46	0.44	0.42	0.40
3	0.61	0.84		0.86	0.77	0.70	0.65	0.61	0.57	0.54	0.51	0.49
4	0.53	0.74	0.88		0.89	0.81	0.75	0.70	0.66	0.63	0.60	0.57
5	0.48	0.66	0.80	0.91		0.91	0.84	0.79	0.74	0.70	0.67	0.64
6	0.44	0.61	0.74	0.84	0.93		0.92	0.86	0.81	0.77	0.73	0.70
7	0.41	0.57	0.68	0.78	0.86	0.94		0.93	0.88	0.83	0.79	0.76
8	0.38	0.53	0.64	0.74	0.81	0.88	0.95		0.94	0.89	0.85	0.81
9	0.36	0.50	0.61	0.70	0.77	0.84	0.90	0.95		0.96	0.92	0.89
10	0.34	0.48	0.58	0.66	0.74	0.80	0.86	0.91	0.96		0.95	0.91
11	0.33	0.46	0.55	0.63	0.70	0.76	0.82	0.87	0.92	0.96		0.96
12	0.32	0.44	0.53	0.61	0.68	0.74	0.79	0.84	0.88	0.93	0.96	

References

Beersma, J.J., Buishand, T.A., 2004. Joint propability of precipitation and discharge deficits in the Netherlands. Water Resour. Res. W12508. http://dx.doi.org/10.1029/2004WR003265.

Bloomfield, J.P., Marchant, B.P., 2013. Analysis of groundwater drought building on the standardised precipitation index approach. Hydrol. Earth Syst. Sci. 17, 4769–4787. http://dx.doi.org/10.5194/hess-17-4769-2013.

Cressie, N.A.C., 1993. Statistics for Spatial Data, Revised Edition. Wiley Series in Probability and Mathematical Statistics. John Wiley & Sons Inc, New York, Chichester, Brisbane, Toronto, Signapore pp. 900.

Diggle, P.J., Ribeiro, P.J. Jr., 2007. Model-Based Geostatistics. Springer Series in Statistics, 228 pp., Springer, New York, USA.

EEA, 2009. Water resources across Europe – confronting water scarcity and drought, EEA Report No. 2/2009. European Environment Agency, Copenhagen.

Hao, Z., Singh, V.P., 2015. Drought characterization from a multivariate perspective: a review. J. Hydrol. 527, 668–678. http://dx.doi.org/10.1016/j.jhydrol.2015.05.031.

Jun, M., Genton, M.G., 2012. A test for stationarity of spatio-temporal random fields on planar and spherical domains. Statistica Sinica 22, 1737–1764. http://dx.doi.org/10.5705/ss.2010.251.

Kao, S.C., Govindaraju, R.S., 2010. A copula-based joint deficit index for droughts. J. Hydrol. 380, 121–134. http://dx.doi.org/10.1016/j.jhydrol.2009.10.029.

Klein Tank, A.M.G., et al., 2002. Daily dataset of 20th-century surface air temperature and precipitation series for the European Climate Assessment. Int. J. of Climatol. 22, 1441–1453. http://dx.doi.org/10.1002/joc.773.

Lloyd-Hughes, B., Saunders, M.A., 2002. A drought climatology for Europe. Int. J. Climatol. 22, 1571–1592. http://dx.doi.org/10.1002/joc.846.

McKee, T.B., N.J. Doeskin, Kleist, J., 1993. The relationship of drought frequency and duration to time scales. In: Proceedings of the 8th Conference on Applied Climatology, January 17–22, Anaheim, California, 179–184.

Nabaltis, I., Tsakiris, G., 2009. Assessment of hydrological drought revisited. Water Resour. Manage. 23, 881–897. http://dx.doi.org/10.1007/s11269-008-9305-1.

Nelsen, R.B., 2006. An Introduction to Copulas. Springer Series in Statistics, 269 pp., Springer, New York, USA.

Palmer, W., 1965. Meteorological drought, Research Paper No. 45, U.S. Department of Commerce Weather Bureau, Washington, D.C.

Renard, B., Lang, M., 2007. Use of a Gaussian copula for multivariate extreme value analysis: some case studies in hydrology. Adv. Water Resour. 30, 897–912. http://dx.doi.org/10.1016/j.advwatres.2006.08.001.

Sims, A.P., Niyogi, D.D.S., Raman, S., 2002. Adopting drought indices for estimating soil moisture: A North Carolina case study. Geophys. Res. Lett. 29, 1183. http://dx.doi.org/10.1029/2001GL013343.

Spinoni, J., Naumann, G., Vogt, J.V., Barbosa, P., 2015. The biggest drought events in Europe from 1950 to 2012. J. Hydrol. Reg. Stud. 3, 509–524. http://dx.doi.org/10.1016/j.ejrh.2015.01.001.

Staudinger, M., Stahl, K., Seibert, J., 2014. A drought index accounting for snow. Water Resour. Res. 50, 7861–7872. http://dx.doi.org/10.1002/2013WR015143.

Svoboda, M., et al., 2002. The drought monitor. Bull. Amer. Meteor. Soc. 83, 1181–1190. http://dx.doi.org/10.1175/1520-0477(2002) 0831181:TDM2.3.CO;2.

van der Schrier, G., Briffa, K.R., Jones, P.D., Osborn, T.J., 2016. Summer Moisture Variability across Europe. J. Clim. 19, 2818–2834. http://dx.doi.org/10.1175/JCLI3734.1.

Wilhite, D., Glantz, M., 1985. Understanding the drought phenomenon: the role of definitions. Water Int. 10, 111–120. http://dx.doi.org/10.1080/02508068508686328.

WMO, 1985. Standardized Precipitation Index – User Guide, WMO No 1090. World Meteorological Organization, Geneva.